The role of direct photolysis in the photodegradation of the herbicide bentazone in natural surface waters

The role of direct photolysis in the photodegradation of the herbicide bentazone in natural surface waters

Luca Carena,[a]* Debora Fabbri,[a] Monica Passananti,[a] Marco Minella,[a] Silvia Berto,[a] Marco Pazzi,[a] Davide Vione[a]

[a] *Dipartimento di Chimica, Università di Torino, Via Pietro Giuria 5, 10125 Torino, Italy.*

*Corresponding author:

E-mail address: luca.carena@unito.it

Telephone: +39-011-6705263

Postal address: Via P. Giuria, 5, 10125 Torino, Italy.

Abstract

The photochemical fate of the herbicide bentazone was assessed by lab experiments and modeling tools. Experimental and modeling results showed that bentazone is mainly photodegraded by direct photolysis in natural water samples, even in the presence of dissolved organic matter (DOM) that can act as light-screening agent, photosensitizer and scavenger of reactive species. Even when it was dissolved in natural water samples containing different DOM amounts, the phototransformation kinetics of bentazone was unchanged compared to irradiation runs in ultrapure water. This finding suggests that the DOM and the other components of our samples did not affect the direct photolysis of bentazone by light-absorption competition, at least at the experimental optical path lengths, and did not induce significant indirect photodegradation by producing reactive transient species. Photochemical modeling in a lake-water photoreactivity scenario corroborated the observed experimental results, showing the predominant role of direct photolysis in the overall (direct + indirect) photodegradation of bentazone at different water depths and DOM contents. However, the model predicted a minor but non-negligible contribution of indirect photochemistry (i.e., reactions triggered by $HO^{\bullet}$, $CO_3^{\bullet-}$ and $^3CDOM^*$) to the herbicide degradation. This contribution (especially

by ^{3}CDOM*) could become crucial in deep and DOM-rich water bodies. Finally, several photoproducts formed by direct photolysis and HO$^{\bullet}$-induced photodegradation were identified, which should not be particularly toxic for aquatic organisms and *Vibrio fischeri* bacteria.

Keywords: Photochemistry; Pesticides; Photochemical modeling; APEX; Photodegradation intermediates.

1. Introduction

Pesticides are widespread micropollutants in surface and groundwaters (Luo et al., 2014; Masiá et al., 2015; Metcalfe et al., 2019), and they cause considerable environmental concern because of their toxic effects on aquatic ecosystems (Ccanccapa et al., 2016; Silva et al., 2015). After application on crops, pesticides can reach groundwaters and surface waters, including streams and lakes, because of leaching and soil runoff processes (Battaglin et al., 2003; Lupi et al., 2019; Milan et al., 2015; Riise et al., 2004). Moreover, water contamination by pesticides is favored by the close link between some crops and the aquatic systems. The latter provide water used for irrigation purposes or, in the case of some paddies, for fish-farming activities (Clasen at al., 2018; Milan et al., 2012). Fortunately, many pesticides are not recalcitrant in water environments and they can be transformed through chemical (e.g., hydrolysis) and biological processes, as well as photochemical reactions in sunlit surface waters (Fenner et al., 2013). Hydrolysis often depends upon water pH and it is faster in acidic and basic conditions, which means that the pH values of natural waters often coincide with a minimum in the hydrolysis kinetics. However, this process can still be an important dissipation pathway for some pesticides (Liu et al., 2001; Ramesh and Balasubramanian, 1999; Tebes-Stevens et al., 2017; Williams and Tjeerdema, 2016). Compared to hydrolysis, biotic and abiotic photochemical degradations usually play a more important role in the environmental fate of

pesticides. Biodegradation is often a key dissipation route (Fenner et al., 2013), but it strongly depends upon the considered xenobiotic and aquatic system (Katagi, 2013). Photochemical reactions may be major transformation pathways for several pesticides and their metabolites (Adachi et al., 2018; Burrows et al., 2002; Konstantinou et al., 2001; Remucal, 2014). These reactions can be distinguished into direct photolysis and indirect photochemistry. Direct photolysis refers to the transformation of a molecule upon direct light absorption. Indeed, some pollutants are able to absorb sunlight, reach excited molecular states and then undergo chemical transformation (Katagi, 2018). Direct photolysis can be inhibited by competitive light-absorbing compounds, including most notably the dissolved organic matter (DOM) that naturally occurs in surface waters. The DOM chromophoric moieties (CDOM) can both screen radiation and act as photosensitizers to trigger the indirect photodegradation of water pollutants. Indeed, upon sunlight absorption CDOM forms the so-called *Photochemically Produced Reactive Intermediates* (PPRIs), which react with water contaminants and cause their degradation. The most important PPRIs are hydroxyl and carbonate radicals ($HO^{\bullet}$ and $CO_3^{\bullet-}$, respectively, which are also generated by the photolysis of nitrate and nitrite), the excited triplet states of CDOM (^{3}CDOM*), as well as singlet oxygen ($^1O_2$) (Vione et al., 2014). Despite their effectiveness in degrading several pollutants including many pesticides (Remucal, 2014), photoreactions yield in some cases photoproducts of considerable environmental concern, which may be toxic to aquatic organisms (Bavcon Kralj et al., 2007; Carena and Vione, 2018; Dong and Hu, 2016). Furthermore, also the biotic degradation processes can be problematic as shown in the case of the herbicide propanil (Carena et al., 2017; Kanawi et al., 2016; Roehrs et al., 2012).

In the present study, the role of direct and indirect photolysis was assessed towards the photodegradation of bentazone (hereinafter BNTZ) in surface water samples. BNTZ is a post-emergence herbicide used in different crops such as wheat, rice and beans, to control weed growth. Because of soil leaching phenomena (Lammoglia et al., 2018), BNTZ has been detected in rivers, coastal waters and groundwaters (Palma et al., 2018; Papadakis et al., 2018; Kock-Schulmeyer et

al., 2019). As shown in previous studies, BNTZ is photolabile in natural waters (coastal lagoon), and it has been degraded in laboratory experiments by 81% via direct photolysis and by 17% via photosensitized processes (Al Housari et al., 2011). In that case, the predicted photochemical lifetime of BNTZ was ~12 days by considering only direct photolysis and $HO^{\bullet}$ reactions (Al Housari et al., 2011). Here we assessed the transformation of BNTZ by all the potentially important photoreaction pathways in fresh waters (direct photolysis, $HO^{\bullet}$ radicals, $^3CDOM^*$, $^1O_2$ and $CO_3^{\bullet-}$; Katagi, 2018; Vione et al., 2014). Moreover, we identified the BNTZ photoproducts formed by the main processes, evaluating their environmental importance by means of photochemical modeling, and assessing the time evolution of acute toxicity.

2. Materials and Methods

2.1 Reagents

Gradient-grade methanol for HPLC analysis was purchased from VWR Chemicals BDH®. All the other compounds were bought from Sigma-Aldrich (analytical grade) and used as received, without further purification. Ultra-pure water was produced by a Milli-Q system (Millipore, 18.2 MΩ cm resistivity, 2 ppb TOC).

The stock solutions of BNTZ (pK_a ~ 3.3 at 24 °C; O'Neil, 2013) were prepared weekly by dissolving the compound in ultra-pure water under magnetic stirring. Their natural acidic pH (<4.5, thereby outside the environmental significance range) was adjusted to 7.0 with NaOH 0.1 mol L^{-1}. The stock solutions were stored in the dark at ~5 °C.

2.2 Lake and paddy water samples

The real water samples used in this work were taken from four small- to medium-sized lakes and a rice field, all located in the Piedmont region (NW Italy). The paddy water was sampled during the

2016 spring season, while the lake water samples were collected in February 2017. After collection, the samples (~1 L) were transported to the lab refrigerated and in the dark. Upon arrival, they were immediately vacuum-filtered with polyamide filters (0.45 µm pore size, Sartorius). The filtered samples were kept in the dark at ~5 °C till the irradiation experiments, to prevent modifications caused by residual biological activity. The origin of the samples and their dissolved organic carbon (DOC) and pH values were as follows: Lake Maggiore (DOC = 0.44 mg_C L^{-1}, pH 6.6), Avigliana Lake (3.1 mg_C L^{-1}, 7.8), Candia Lake (4.0 mg_C L^{-1}, 7.5), Viverone Lake (4.1 mg_C L^{-1}, 7.5), Santhià rice-field (2.4 mg_C L^{-1}, 7.3). The absorption spectra of the natural water samples are shown in **Fig. SM-1** in the Supplementary Material (SM).

2.3 Irradiation experiments

Spiked solution aliquots (20 mL, 20 µmol L^{-1} BNTZ) in both ultra-pure water adjusted to pH 7.0 and real water samples were irradiated in cylindrical Pyrex glass cells, under a Philips TL K05 lamp (40 W) that mainly emits UVA radiation. The rationale for using this lamp was the following: *(i)* BNTZ mostly absorbs radiation in the UV region, thus most of its photochemistry would take place where the lamp emits; *(ii)* the majority of the photoprocesses triggered by sunlit CDOM take place in the UV and especially the UVA region (see SM for details). The chosen initial BNTZ concentration was the lowest that still allowed for reliable quantification by liquid chromatography (*vide infra*). This concentration level was also low enough to avoid self-sensitization processes (photodegradation of a compound, triggered by the excited states of the same molecule; Bedini et al., 2012).

The UV irradiance of the lamp (12.3 ± 0.9 W m^{-2} in the 290-400 nm range) was measured with an irradiance meter by CO.FO.ME.GRA. (Milan, Italy). The solutions were magnetically stirred during irradiation. A detailed description of the irradiation system can be found in the SM of Carena et al. (2017).

127 The lamp radiation reached the solutions mainly from the top. However, to properly take into
128 account the multiple reflection phenomena that typically occur in photoreactors, chemical
129 actinometry was used to measure the spectral photon flux density in solution. 2-Nitrobenzaldehyde
130 (2NBA, 100 μmol L^{-1} initial concentration) was used as chemical actinometer (Galbavy et al., 2010;
131 Marchisio et al., 2015; Willet and Hites, 2000). The detailed method has been reported by
132 Marchisio et al. (2015). The 2NBA solutions were irradiated in the same cells used for BNTZ
133 irradiation, under the same lamp and using the same irradiation volume.
134 **Fig. SM-2** shows the spectral photon flux density of the used lamp, together with the UV-visible
135 absorption spectrum of BNTZ. The two spectra overlap between 300 and 390 nm, which is also the
136 spectral range where BNTZ absorbs sunlight. The BNTZ photodegradation profiles followed
137 pseudo-first order kinetics (note that the reactions with PPRIs follow second-order kinetics, but
138 PPRIs themselves are in steady-state; their concentrations being constant during irradiation, the
139 second order reduces to a pseudo-first order). The time trends were fitted with the equation C_t =
140 $C_o \cdot \exp(-k' \cdot t)$. Here, k' is the experimental pseudo-first order degradation rate constant, calculated by
141 fitting the relevant degradation curves, t is the irradiation time, C_o the initial BNTZ concentration
142 (20 μmol L^{-1}), and C_t the BNTZ concentration at the irradiation time t. The initial degradation rates
143 of BNTZ were computed as $R = k'C_o$.
144 To quantify the BNTZ concentration at each scheduled irradiation time (C_t), solutions aliquots (1.2
145 mL) were sampled through the lateral neck of the glass cells, which were otherwise kept tightly
146 closed during irradiation. Aliquots were then analyzed by High-Performance Liquid
147 Chromatography coupled with Diode Array Detection (HPLC-DAD, *vide infra*). In order not to
148 affect too much the initial optical depth (1.6 cm), each solution was sampled only twice causing ~
149 12% maximum volume variation. This is well within the typical variability of this kind of
150 experiments.

151 The kinetic assessment of the dark BNTZ degradation (blank experiments) caused by, e.g.,
152 hydrolysis and/or biodegradation was carried out by placing both synthetic and real water samples,
153 spiked with BNTZ, in glass cells wrapped with double aluminum foil, under the irradiation lamp.
154 The rationale for placing them under the lamp was to achieve comparable temperature and stirring
155 conditions as for the irradiated samples.
156 All the irradiation experiments were carried out in duplicate, and the data points were then plotted
157 as average values plus-or-minus the standard error.
158

159 **2.4 Identification of the BNTZ photoproducts**

160 Aqueous BNTZ solutions (1 mmol L^{-1}) at pH 7 were irradiated inside a total of three cylindrical
161 Pyrex glass cells as reported in paragraph 2.3. Analysis by Gas Chromatography-Mass
162 Spectrometry (GC-MS) then followed, after SPME (Solid Phase Micro-Extraction) of samples at
163 different irradiation times (t = 0, 24h, 48h and 72h). The sample solutions (total pooled volume of
164 60 mL) were divided into three aliquots of 20 mL each, and the pH was adjusted to 4, 7 and 10. The
165 goal was to maximize the SPME extraction of photoproducts with different acid-base properties.
166 The SPME procedure was as follows: a DVB/CAR/PDMS, 57914-U fiber was immersed into the
167 sample solution at 24 ˚C under magnetic stirring. After 30 min, the fiber was introduced into the GC
168 injector where the adsorbed compounds were thermally desorbed and injected into the GC column
169 (ZB-624, 30 m length, 0.25 mm ID, 1.4 μm Film Thickness).
170 A similar procedure was applied to identify the indirect photoproducts of BNTZ. In this case, an
171 aqueous solution of bentazone (1 mmol L^{-1}) and H_2O_2 (0.1 mol L^{-1}) at pH 7 was exposed to light as
172 reported in paragraph 2.3, and analyzed by SPME GC-MS as before (including the pH adjustment
173 to 4, 7 and 10), after 0h, 4h, 16h and 30h of irradiation. H_2O_2 was used as $HO^{\bullet}$ source, and the
174 irradiated solutions containing H_2O_2 in ultra-pure water are virtually free of $^3CDOM^*$ and $CO_3^{\bullet-}$ as
175 potentially interfering PPRIs.

176

177 **2.5 Assessment of the BNTZ toxic effects with experimental (*Vibrio fischeri*) and *in-silico***
178 **methods**

179 The assessment of the toxicity towards aquatic microorganisms of both BNTZ and its
180 photoproducts was carried out experimentally by using *Vibrio fischeri* bacteria, and *in silico* by
181 QSAR modeling.

182 Acute toxicity of samples collected at different irradiation times was evaluated with a Microtox
183 Model 500 Toxicity Analyzer (Milan, Italy). This assay exploits the bioluminescence changes of the
184 marine bacterium *Vibrio fischeri* by monitoring the inhibition in the natural emission of the
185 luminescent bacteria when challenged with toxic compounds. Freeze-dried bacteria, reconstitution
186 solution, diluent (2% NaCl) and an adjustment solution (non-toxic 22% sodium chloride) were
187 obtained from Azur (Milan, Italy). Samples were tested in a medium containing 2% sodium
188 chloride, and luminescence was recorded after 5, 15 and 30 min of incubation at 15 °C. No
189 substantial differences were found between the three contact times. Inhibition of luminescence,
190 compared with a toxic-free control to give the percentage inhibition, was calculated following the
191 established protocol and using the Microtox calculation program.

192 QSAR modeling was performed by means of the freely available ECOSAR V2.0 software
193 [Ecological Structure Activity Relationships (ECOSAR) Class Program], developed by the U.S.
194 Environmental Protection Agency (EPA) (Mayo-Bean et al., 2012). ECOSAR computes both acute
195 (LC_{50} and EC_{50}) and chronic (ChV = Chronic Value) toxicity parameters toward aquatic organisms
196 on the basis of the molecular structure of the considered neutral organic compound. In particular,
197 toxicity outputs are fish 96h - LC_{50}, daphnid 48h – LC_{50} and green algae 96h – EC_{50}. In contrast, the
198 ChV is computed as the geometric mean of NOEC (no-observed-effect concentration) and LOEC
199 (lowest-observed-effect concentration) (Mayo-Bean et al., 2012). Furthermore, the computed LC_{50},
200 EC_{50} and ChV values related to Log K_{ow} > 5, > 6.4 and > 8, respectively, were here neglected
201 (Mayo-Bean et al., 2017a).

202

203 **2.6 HPLC-DAD, GC-MS, DOC, pH and UV-Vis absorption measurements**

204 The HPLC-DAD instrument used to quantify BNTZ during the irradiation experiments was a
205 VWR-Hitachi LaChrom Elite chromatograph equipped with L-2200 autosampler (injection volume
206 60 µL), L-2130 quaternary pump for low-pressure gradients, Duratec vacuum degasser, L-2300
207 column oven (set at 40 °C), and L-2455 photodiode array detector. The column was a VWR
208 LiChroCART 125-4 Cartridge, packed with LiChrospher 100 RP-18 (125mm×4mm×5µm). Elution
209 was carried out in isocratic mode with a mixture of 58% ultrapure water (acidified at pH ~2.8 with
210 phosphoric acid) and 42% methanol, with a total flow rate of 1.0 mL min^{-1} (column dead time ~1.0
211 min). The BNTZ elution time was 8.9 min and the detection wavelength was 221 nm.
212 GC-MS analytical determinations were performed using an Agilent 6890N Network GC System
213 coupled with an Agilent 5973 Inert Mass Spectrometer, operating in the electron impact ionization
214 mode. Source was kept at a temperature of 270 °C. The oven temperature was programmed as
215 follows: initial column temperature was 40 °C for 5 min, then increased by 15 °C min^{-1} to 260 °C,
216 and finally keeping it steady at 260 °C for 8.33 min, for a total run time of 28 min. The carrier gas
217 was ultra-pure He (1.0 mL min^{-1}; SIAD, Bergamo, Italy). Full mass spectra were acquired from m/z
218 29 to m/z 500.
219 The total dissolved organic carbon (DOC) of lake and paddy water samples was determined by
220 using a Shimadzu TOC-VCSH instrument, equipped with an ASI-V autosampler. The DOC was
221 calculated as the difference between total (dissolved) carbon (TC) and inorganic carbon (IC).
222 The pH of the samples was measured with a combined glass electrode, connected to a Metrohm 602
223 pH meter.
224 The UV-Vis absorption spectra of the lake and paddy water samples were measured with a V-550
225 Jasco spectrophotometer, using a 5.0 cm optical path quartz cuvette (Hellma).
226

2.7 Photochemical modeling

The photochemical fate of BNTZ in environmental waters (namely, its pseudo-first order photodegradation rate constants and the corresponding half-life times) was modeled with the APEX software (Bodrato and Vione, 2014). APEX can model the direct and indirect photochemistry of pollutants in well-mixed surface waters, such as the whole water column of lakes during overturn, but also their epilimnion during summer stratification, and even the floodwater of rice fields (e.g. Carena and Vione, 2018).

Briefly, APEX requires as input data the chemical and photochemical features of the water body (i.e., concentration of photosensitizers and scavengers of the PPRIs, water absorption spectrum and water depth), as well as the photoreactivity parameters of the considered xenobiotic (i.e., the UV-visible absorption spectrum, the direct photolysis quantum yield and the second-order rate constants for the reactions with the different PPRIs). **Table SM-2** shows the relevant parameters of BNTZ photoreactivity used in the modeling. The output values of the photodegradation kinetics are averaged over the entire water column depth.

Here, the software was run supposing a clear-sky scenario corresponding to July 15th at 45°N latitude. The corresponding time unit (default in APEX), the so-called Summer Sunny Day (SSD), is equivalent to 10h of continuous irradiation at 22 W m^{-2} UV irradiance under clear-sky sunlight.

3. Results and Discussion

3.1 BNTZ photodegradation and its photochemical modeling

Fig. 1a shows the experimental degradation profiles of BNTZ under irradiation. No dark degradation of BNTZ was observed (data not shown) in either ultrapure water or lake/paddy water samples. This finding agrees with previous works showing no BNTZ hydrolysis or biodegradation, in either synthetic or real water samples (Al Housari et al., 2011; Song et al., 2019; Zeng and

Arnold, 2013). No significant difference between the BNTZ direct photolysis in ultrapure water and its phototransformation in natural waters was observed. The BNTZ photodegradation rate in natural water samples (R_{DOM}) and that in ultrapure water (R_{H2O}) yielded R_{DOM} = 0.90-0.95 R_{H2O} (see **Fig. 1b**). Several previous works have shown that some pollutants undergo inhibition of direct photodegradation in the presence of DOM, basically because of competition for irradiance with the chromophoric DOM moieties (CDOM) (e.g., Dimou et al., 2004; Malouki et al., 2004; Walse et al., 2004). To assess the possible role of light screening by CDOM on BNTZ photodegradation, the ratio between the photon absorption rate of BNTZ in both real samples ($P_{a,DOM}$) and ultrapure water ($P_{a,H2O}$) was computed as follows (**Eq.1**):

$$\frac{R_{DOM}}{R_{H2O}} = \frac{P_{a,DOM}}{P_{a,H2O}} = \frac{\int_{\lambda 1}^{\lambda 2} p^0(\lambda) \frac{A_{\lambda,BNTZ}}{A_{\lambda,tot}} [1 - 10^{-A_{\lambda,tot}}] d\lambda}{\int_{\lambda 1}^{\lambda 2} p^0(\lambda) [1 - 10^{-A_{\lambda,BNTZ}}] d\lambda} \qquad (Eq.1)$$

where $p^0(\lambda)$ is the spectral photon flux density of the lamp in solution (**Fig. SM-2**), while $A_{\lambda,BNTZ}$ and $A_{\lambda,tot}$ are the Lambert-Beer absorbance values of, respectively, BNTZ and the whole irradiated solution (*i.e.*, $A_{\lambda,tot} = A_{\lambda,CDOM} + A_{\lambda,BNTZ}$). The choice of λ_1 and λ_2 was linked to the spectral-range overlap of lamp emission and BNTZ absorption (300-392 nm).

The theoretical values of R_{DOM} $(R_{H2O})^{-1}$ calculated with **Eq. (1)** are reported in **Fig. 1b** (blue bars), showing 1-5% difference with the experimental ratios (yellow bars). This difference is well within the typical uncertainty of the irradiation technique. Therefore, at least at the optical path lengths of the irradiation experiments BNTZ was mainly degraded by direct photolysis, and it can be safely assumed that light screening by CDOM can account for the small differences between ultra-pure and natural water samples.

However, UV radiation that illuminates laboratory solutions, and that is efficiently absorbed by both CDOM and several organic compounds such as BNTZ, poorly penetrates in real deep water columns in the presence of CDOM (Bracchini et al., 2004; Rose et al., 2009).

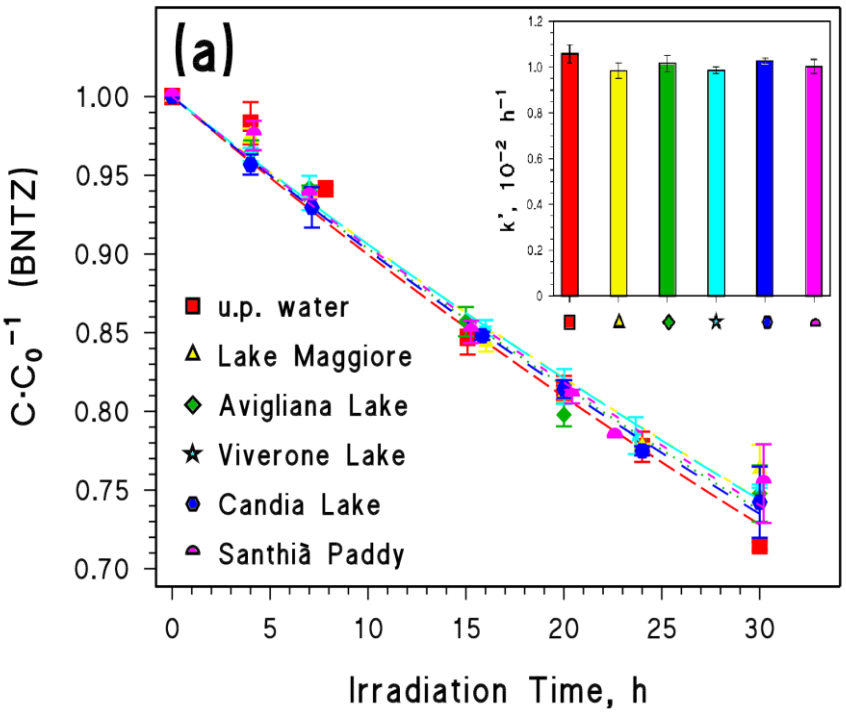

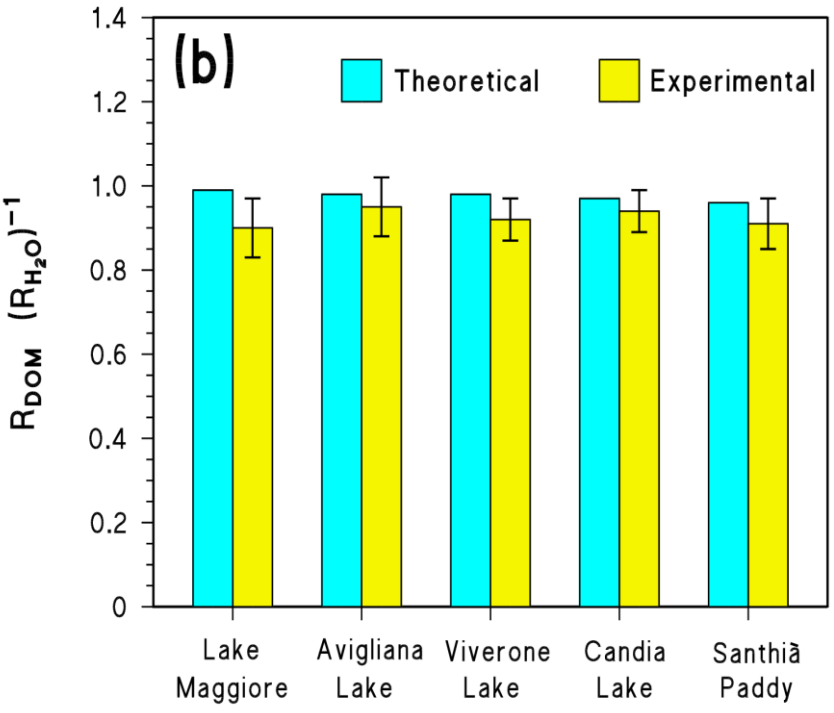

Fig. 1. (a) BNTZ photodegradation profiles in different aqueous matrices. Inset: experimental k' values for BNTZ photodegradation. (b) DOM-induced inhibition (light screening) of BNTZ photodegradation assessed as both theoretical and experimental ratio between the BNTZ degradation rate in real water samples and in ultrapure water ('u.p. water').

In contrast, visible light penetrates more deeply in water and it is absorbed by CDOM as well, thereby increasing the importance of CDOM-related photoprocesses (including ^{3}CDOM* reactions) vs. direct photolysis in deep water bodies (Canonica, 2007; McNeill and Canonica, 2016). Consequently, the relative importance of the ^{3}CDOM* reactions is often higher in the natural environment than in laboratory irradiation systems, because of differences in the water column depth and the related optical path length (Bianco et al., 2015; **Fig SM-4**). Therefore, because the second-order rate constant of the reaction between BNTZ and ^{3}CDOM* has been estimated to be quite high with steady-state irradiations experiments in real water samples (Zeng and Arnold, 2013; see also **Table SM-2**), ^{3}CDOM* could play an important role in the overall phototransformation of BNTZ. Because elevated water depths are hardly accessible to experimentation, it is interesting to model the photochemical behavior of BNTZ in natural water bodies.

The modeling of BNTZ photodegradation in lake water (3 m lake water depth, 15th of July at 45°N) agrees reasonably well with the experimental findings (**Fig. 2a**). The direct photolysis is predicted to be the main phototransformation pathway of the herbicide, while the roles of $HO^\bullet$ and $CO_3^{\bullet-}$ are quite low between 1 and 5 mg_C L^{-1}. The importance of $HO^\bullet$ and $CO_3^{\bullet-}$ reactions becomes even negligible for DOC > 5 mg_C L^{-1}. $^1O_2$ is not important as well in our scenario, although $^1O_2$ can be the major PPRI photodegrading BNTZ in prairie potholes with high DOM content between 20 and 38 mg_C L^{-1}. In these environments, direct photolysis is limited to 40-45% of the total BNTZ photodegradation (Zeng and Arnold, 2013). According to our model results, at so high DOC levels the main role in BNTZ degradation would be played by ^{3}CDOM* instead of $^1O_2$, which is expected to give a minor contribution to the process. The main reason for this difference could be due to the fact that CDOM in prairie potholes has very different photoreactivity than that assumed by the APEX software, which has been designed around lake-water CDOM and its photoreactivity.

Coming back to the modeled lake-type environment (**Fig. 2**), the results also suggest that BNTZ could be significantly degraded by ^{3}CDOM* at DOC > 2 mg_C L^{-1}. This makes a difference with the

irradiation experiments, where lake/paddy water from Avigliana, Viverone, Candia and Santhià had DOC > 2 mg_C L^{-1}. However, the optical path length of the irradiated samples was much shorter (1.4 - 1.6 cm) than the water column depths found in the most reasonable environmental scenarios, including the modeled one. We can thus speculate that differences in water-column depth may account for the different relative roles of direct photolysis and ^{3}CDOM* reaction between model output and experimental results. Indeed, by lowering the water depth to 1.5 cm (**Fig. 2b**), which is comparable to the optical path length of our experiments, the direct photolysis assumes much higher importance than in the 3-m depth scenario. The model still predicts some minor role for $HO^{\bullet}$, $CO_3^{\bullet-}$ and ^{3}CDOM* in BNTZ degradation, which might or might not be highlighted experimentally given the uncertainties in both model results and irradiation runs. The fact that the irradiation experiments seem to exclude a significant role of indirect photochemistry (**Fig. 1b**) may have the following explanations: *(i)* the importance of indirect photoreactions is comparable to the experimental uncertainty, and it is thus not or hardly appreciable; *(ii)* the CDOM photoreactivity assumed in the model (average freshwater conditions) is higher compared to that of the studied samples; *(iii)* DOM inhibits the BNTZ degradation because of back-reduction processes due to its intrinsic antioxidant activity (Canonica and Laubscher, 2008; Leresche et al., 2016; Wenk and Canonica, 2012). However, the indirect photochemistry of ^{3}CDOM* could become the main BNTZ phototransformation pathway in a deep water body with a high DOM content (DOC = 10 mg_C L^{-1}, depth > 3 m, see **Fig. SM-4**). In that case, the BNTZ direct photolysis would be overcome by ^{3}CDOM* photochemistry because of the light penetration issues explained above. However, in deep and DOM-rich water bodies the photoreaction kinetics would be quite slow, and other non-photoinduced processes could become important or even dominate the degradation of BNTZ.

The reactions with $HO^{\bullet}$ and $CO_3^{\bullet-}$ could be the second most important photodegradation pathway of BNTZ at low DOC. Their importance could be increased in the presence of elevated nitrate and/or nitrite concentration values (see **Fig. SM-5**).

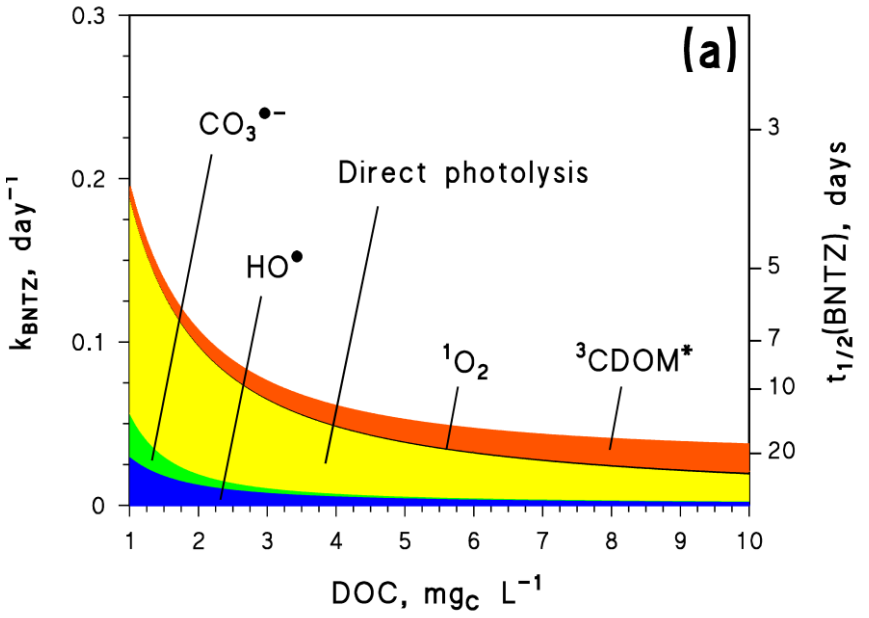

334

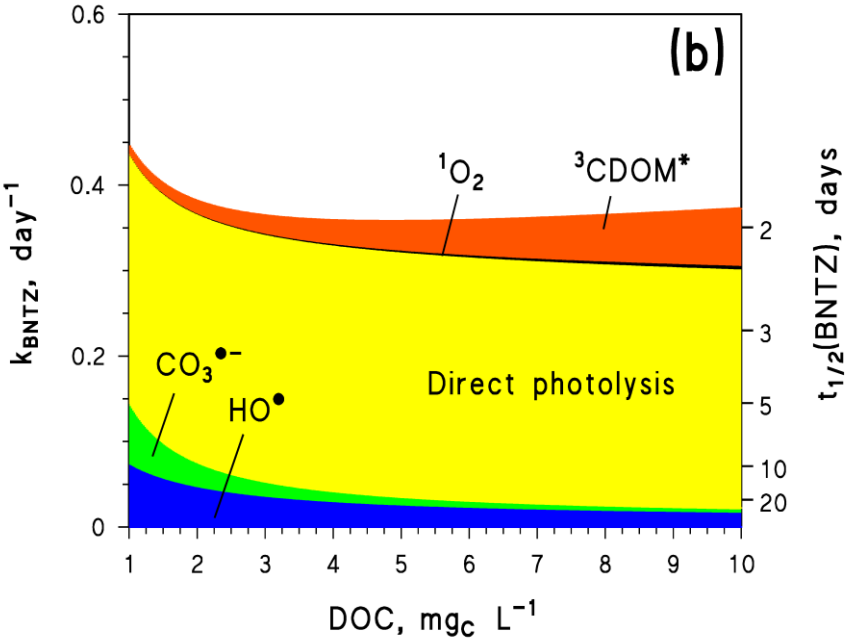

335

336

337 **Fig. 2.** Pseudo-first order rate constants (left Y-axis) and half-life times (right Y-axis) of BNTZ in a lake
338 water column of (a) 3 m and (b) 1.5 cm depth. The assumed water chemical composition was: 100 µmol L^{-1}
339 NO_3^-, 1 µmol L^{-1} NO_2^-, 1 mmol L^{-1} HCO_3^-, and 10 µmol L^{-1} CO_3^{2-}. The day time unit refers to fair-weather
340 15 July at 45°N latitude.

341

342 Our model results agree well with the reported photochemical half-life time of BNTZ, which has
343 been predicted by Al Housari et al. (2011) to be ~12 days in a coastal lagoon on the basis of
344 irradiation experiments. In the same work, field data suggested the BNTZ lifetime to be about 5-15
345 days, which is compatible as well with the range predicted by APEX (**Fig. 2a**). Because BNTZ
346 biodegradation can be slow (Al Housari et al., 2011; Song et al., 2019), and because we did not
347 observe significant BNTZ degradation in natural waters in the dark, we can predict that
348 photochemistry (and in particular the direct photolysis) could play an important role in the total
349 BNTZ dissipation in lake water.
350

351 **3.2 BNTZ degradation products**

352 GC-MS analyses were carried out on irradiated solutions of BNTZ to identify the photoproducts.
353 Their characterization may provide further information about the transformation mechanisms of the
354 herbicide, and it can also be useful to assess and explain the time trend of toxicity. Indeed, it has
355 been shown for some pollutants that the degradation products may be more persistent and toxic than
356 the parent compound (Bavcon Kralj et al., 2007; Erickson et al., 2012; Isidori et al., 2009;
357 Passananti et al., 2015; Vogna et al., 2004). This issue is often underestimated, but it should be
358 taken into account in order to properly assess the environmental impact of a pollutant.
359 The products derived by direct and indirect photolysis were identified by GC-MS. Some
360 photoproducts were identified in all the extraction conditions (pH 4, 7 and 10), while others were
361 adsorbed on the fiber only at specific pH values.
362 **Fig. 3** shows the possible molecular structures of the BNTZ photodegradation products in pure
363 water and in the presence of $HO^{\bullet}$ radicals, generated by H_2O_2 photolysis, proposed on the basis of
364 the GC-MS analysis. The rationale for the choice of the two processes is that direct photolysis is the
365 main BNTZ photoreaction, while $HO^{\bullet}$ may play an important role at low DOC and low water depth,
366 where photoreactions are fast and thus very competitive with additional processes (**Fig. 2a**). The
367 compounds detected in both conditions (direct and indirect photolysis) are highlighted in red. The

368 main BNTZ photoproduct observed after 72h of irradiation (direct photolysis) is the
369 photohydrolysis compound **1a**, derived by the cleavage of the amide N-S and amine N-S bonds.
370 This compound has been identified previously as a BNTZ degradation product (Nilles and Zabik,
371 1975; Song et al., 2019), and its formation generates sulfuric acid that could further catalyze
372 degradation reactions. 2-Amino-*N*-isopropylbenzamide (**1a**) may absorb light and undergo a
373 Norrish type II reaction to produce the benzamide **3a** (White et al., 1996). A di-radical species
374 photogenerated by **1a** could also produce compound **4b**, as well as the bicyclic compound **5b**
375 through an intramolecular reaction. Also the bicycle **2a** could derive from **1a** via intramolecular
376 recombination with the isopropyl chain and further oxidation. Finally, the oxidation of the aromatic
377 amine may lead to the nitroderivative **6b**.
378 The irradiation of BNTZ in the presence of H_2O_2 (indirect photolysis) for 30h yielded several
379 products, some of which (**1a**, **2a** and **3a**) were also observed in direct photolysis. Except for *N*-
380 methylbentazone (**4c**), all the detected compounds do not contain sulfur in the molecular structure.
381 This finding suggests that photohydrolysis to **1a** is the main degradation pathway also in the case of
382 $HO^{\bullet}$. However, we cannot exclude the possibility that compound **1a** actually derives from BNTZ
383 direct photolysis rather than exclusively from the $HO^{\bullet}$-induced reactions. Indeed, although the H_2O_2
384 concentration was 100-fold higher than that of BNTZ, the molar absorption coefficient of the latter
385 species is nevertheless higher of the same order of magnitude. Therefore, BNTZ absorbs light at
386 least as well as H_2O_2, and in irradiated H_2O_2 solutions its direct photolysis can occur at the same
387 time as degradation by $HO^{\bullet}$. Another evidence of the loss of sulfur from BNTZ was the solution pH
388 decrease from 7 to 4 during light exposure, presumably because of the formation of H_2SO_4. These
389 findings are quite in contrast with the results obtained by Peschka et al. (2007), who have not
390 observed the loss of sulfur from BNTZ during irradiation in water enriched with inorganic salts and
391 organic matter. N-methylbentazone (**4c**) has been already identified as a transformation product of
392 BNTZ by Song et al. (2019), during irradiation of water/methanol and water/ethyl acetate solutions.
393 Those conditions could have allowed the BNTZ methylation by the solvent itself.

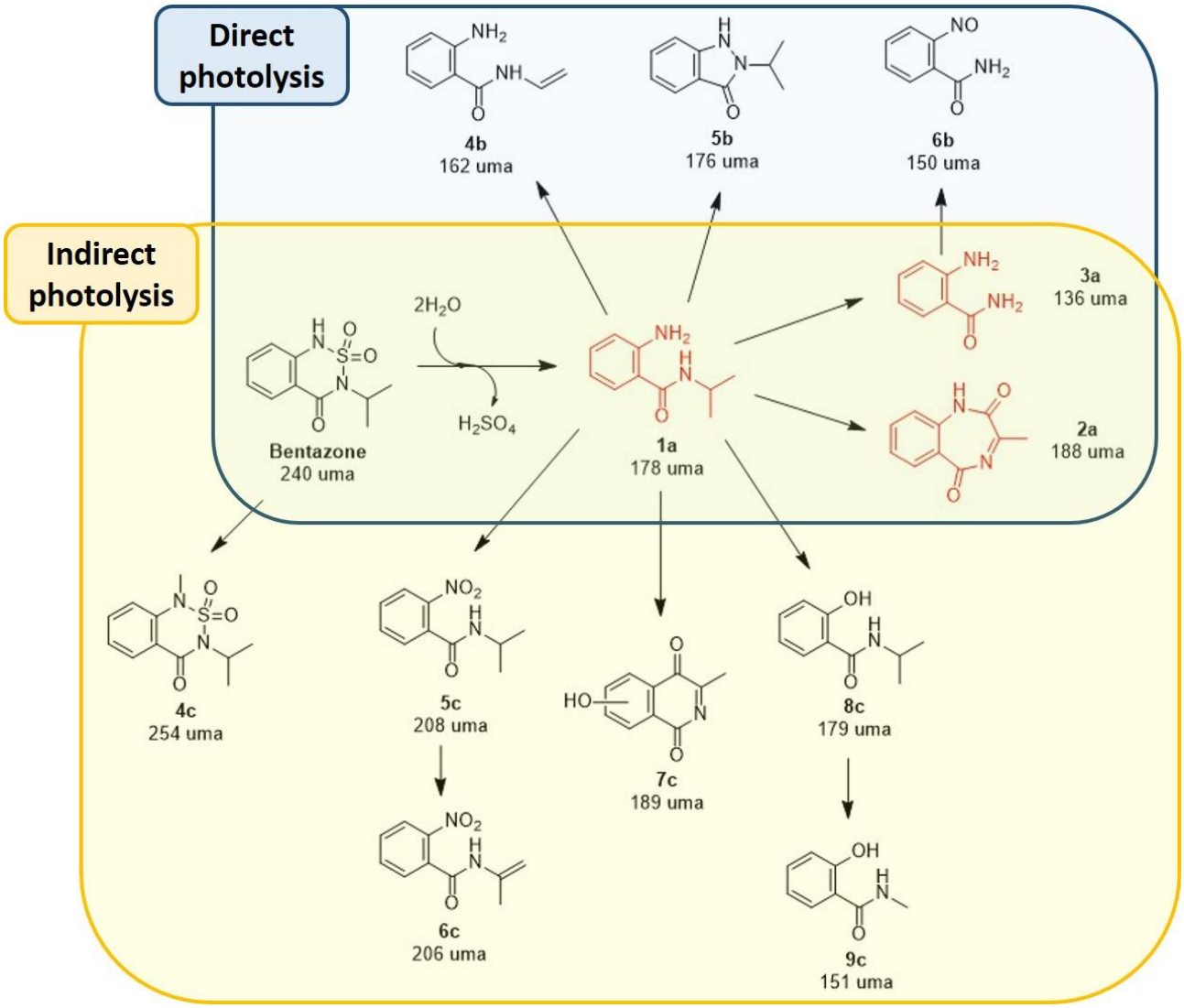

Fig. 3. Possible degradation pathways of BNTZ under UV irradiation in water (inside the blue box, direct photolysis) and in the presence of UV + H_2O_2 (inside the yellow box, indirect photolysis by $HO^{\bullet}$). The products included in the overlapping area of the yellow and blue boxes, highlighted in red for higher clarity, were observed in both conditions. The recorded mass spectra are reported in the SM (from **Fig. SM-7 to Fig. SM-10**).

In our case, however, BNTZ was irradiated in water (without organic solvent) at quite a high concentration (1 mmol L^{-1}). Such conditions might perhaps trigger some cross-reactions between different BNTZ molecules, leading to the formation of **4c**. Consequently, the formation of **4c** in our samples might be an artifact and it should be still verified in environmentally relevant conditions, where BNTZ occurs at lower concentration values. To our knowledge, compounds **6c**, **7c** and **9c** have never been identified as products of BNTZ degradation, and they have thus been observed in this work for the first time.

It has already been reported in the literature that **5c** and **8c** are BNTZ transformation products obtained under photolytic (Nilles and Zabik, 1975), photocatalytic (UV + TiO_2) and $HO^{\bullet}$-induced degradation conditions (Mir et al., 2014; Guelfi et al., 2019). Product **5c** derives from the oxidation of the aromatic amine group, while the substitution of this latter with OH could lead to **8c**. In particular, **6c** and **9c** could derive from **5c** and **8c,** respectively, upon transformation of the isopropyl chain. Subsequent oxidation of **1a** could lead to the bicycle **7c** that is stabilized by resonance. Finally, we did not observe BNTZ dimerization products as in previous works (Berberidou et al., 2017; Eyheraguibel et al., 2009; Nilles and Zabik, 1975), probably due to our analysis conditions. Indeed, the BNTZ retention time was 25.6 min and the total chromatographic run time was 28 min. Therefore, since dimerization products should have higher retention time compared to BNTZ, it is reasonable that we did not observe these products. Our goal was to identify the BNTZ degradation products rather than the large dimerization products, which are usually less important under environmental conditions because their formation requires substrate concentration values higher than those occurring in surface waters.

3.3 Toxicity assessment of BNTZ photoproducts towards aquatic organisms

The LC_{50}/EC_{50} and ChV parameters towards aquatic organisms were evaluated for BNTZ and the identified photoproducts reported in **Fig. 3** with the ECOSAR software. When considering the same chemical class as the parent compound, no formation of peculiarly toxic intermediates was

predicted during either direct or HO•-induced photodegradation (**Table SM-3**). Note that when using ECOSAR, the difference of toxicity between two compounds can be deemed significant when the predicted values differ by at least one order of magnitude (Mayo-Bean et al., 2012). It should be pointed out that some molecules (i.e., **1a**, **5b**, **8c** and **9c**) also belong to different chemical classes than BNTZ, because photodegradation introduces further functional groups. Actually, some toxicity parameters relative to hydrazines and phenol amines satisfied the above rule of increased toxicity. However, when using the traditional approach that considers only the chemical class with the most conservative effect level (Mayo-Bean et al., 2017b), an important toxicity increase seems to be ruled out.

The measurements with *Vibrio fischeri* did not show important acutely toxic effects of either BNTZ or its photodegradation mixtures after 4, 16 and 23h of irradiation at the adopted initial BNTZ concentration (20 μmol L^{-1}, **Fig. SM-6**). Our findings are quite different from those reported by Berberidou et al. (2017), which observed an increase of toxicity towards *Vibrio fischeri* during the early stages of the BNTZ photocatalytic degradation. This probably because direct photolysis and photocatalytic degradation of the compound proceed with different mechanisms, and because we adopted a lower BNTZ concentration. Therefore, both *in-silico* methods and experimental assessments suggest that BNTZ photodegradation does not yield toxic species. The reason might be that *(i)* the detected intermediates are not particularly toxic, including **1a**, **5b**, **8c** and **9c**, or *(ii)* toxic compounds are formed at very low concentration.

Although both models and experiments suggest that the BNTZ photoproducts are not more toxic than the parent compound, at least at the formed concentration values, further and more sensitive toxicological assessments should be carried out in order to ensure that photodegradation really leads to BNTZ attenuation.

4. Conclusion

Direct photolysis is here shown to be the main photolytic pathway for BNTZ in natural water samples. The prevalence of direct photolysis was confirmed by photochemical modeling, and it should be more marked if the water body is shallow. The computed half-life time agreed well with the values reported in the literature for field conditions, thereby suggesting that the direct photolysis can be the major dissipation pathway for BNTZ in most surface waters. Indirect photochemistry might play a non-negligible role, both in shallow and DOM-poor waters where $HO^{\bullet}$-induced reactions are important, or in deep and DOM-rich waters, where $^{3}CDOM^{*}$ could become the main actor in BNTZ photodegradation. However, in the latter case photodegradation is predicted to be quite slow, and additional reaction pathways (e.g., biodegradation) could take on a major importance.

Several BNTZ photoproducts were identified for the direct photolysis and the $HO^{\bullet}$-induced transformation of the herbicide, thereby allowing for the proposal of a photodegradation pathway. Important toxic effects of the detected photoproducts towards aquatic organisms and *Vibrio fischeri* bacteria could be excluded, with the use of QSAR modeling and toxicity tests.

Acknowledgements

LC acknowledges Compagnia di San Paolo (Torino, Italy) for financially supporting his PhD fellowship.

Declarations of interest: none

References

Adachi, T., Suzuki, Y., Nishiyama, M., Kodaka, R., Fujisawa, T., Katagi, T., 2018. Photodegradation of Strobilurin Fungicide Mandestrobin in Water. *J. Agric. Food Chem*. 66, 8514-8521. DOI: 10.1021/acs.jafc.8b03610.

Al Housari, F., Höhener, P., Chiron, S., 2011. Factors responsible for rapid dissipation of acidic herbicides in the coastal lagoons of the Camargue (Rhône River Delta, France). *Sci. Total Environ*. 409, 582-587. DOI: 10.1016/j.scitotenv.2010.10.036.

Battaglin, W. A., Thurman, E. M., Kalkhoff, S. J. and Porter, S. D., 2003. Herbicides and transformation products in surface waters of the midwestern United States. *J. Am. Water Resour. As.* 39, 743-756. DOI: 10.1111/j.1752-1688.2003.tb04402.x.

Bavcon Kralj, M., Franko, M., Trebše, P., 2007. Photodegradation of organophosphorus insecticides - Investigations of products and their toxicity using gas chromatography-mass spectrometry and AChE-thermal lens spectrometric bioassay. *Chemosphere* 67, 99-107. DOI: 10.1016/j.chemosphere.2006.09.039.

Bedini, A., De Laurentiis, E., Sur, B., Maurino, V., Minero, C., Brigante, M., Mailhot, G., Vione, D., 2012. Phototransformation of anthraquinone-2-sulphonate in aqueous solution. Photochem. Photobiol. Sci. 11, 1445-1453.

Berberidou, C, Kitsiou, V., Kazala, E., Lambropoulou, D. A., Kouras, A., Kosma, C. I., Albanis, T. A., Poulios, I., 2017. Study of the decomposition and detoxification of the herbicide bentazon by

heterogeneous photocatalysis: Kinetics, intermediates and transformation pathways. *Appl. Catal. B-Environ.* 200, 150-163. DOI: 10.1016/j.apcatb.2016.06.068.

Bianco, A., Fabbri, F., Minella, M., Brigante, M., Mailhot, G., Maurino, V., Minero, C., Vione, D., 2015. New insights into the environmental photochemistry of 5-chloro-2-(2,4-dichlorophenoxy)phenol (triclosan): Reconsidering the importance of indirect photoreactions, *Water Res.* 72, 271-280. DOI: 10.1016/j.watres.2014.07.036.

Bodrato, M., Vione, D., 2014. APEX (Aqueous Photochemistry of Environmentally occurring Xenobiotics): A free software tool to predict the kinetics of photochemical processes in surface waters. *Environ Sci-Proc Imp* 16, 732-740. DOI: 10.1039/C3EM00541K.

Bracchini, L., Cózar, A., Dattilo, A. M., Falcucci, M., Gonzales, R., Loiselle, S., Hull, V., 2004. Analysis of extinction in ultraviolet and visible spectra of water bodies of the Paraguay and Brazil wetlands. *Chemosphere* 57, 1245-1255. DOI: 10.1016/j.chemosphere.2004.08.050.

Burrows, H. D., Canle L, M., Santaballa, J. A., Steenken, S., 2002. Reaction pathways and mechanisms of photodegradation of pesticides. *J. Photochem. Photobiol. B-Biol.* 67, 71-108. DOI: 10.1016/S1011-1344(02)00277-4.

Canonica, S., 2007. Oxidation of Aquatic Organic Contaminants Induced by Excited Triplet States. *Chimia* 61, 641-644. DOI: 10.2533/chimia.2007.641.

Canonica, S., Laubscher, H. U., 2008. Inhibitory effect of dissolved organic matter on triplet-induced oxidation of aquatic contaminants. *Photochem. Photobiol. Sci*. 7, 547–551. DOI: 10.1039/b719982a.

Carena., L., Minella, M., Barsotti, F., Brigante, M., Milan., M., Ferrero, A., Berto, S., Minero, C., Vione, D., 2017. Phototransformation of the Herbicide Propanil in Paddy Field Water. *Environ. Sci. Technol.* 51, 2695-2704. DOI: 10.1021/acs.est.6b05053.

Carena, L., Vione, D., 2018. Modelling the photochemistry of imazethapyr in rice paddy water, *Sci. Total Environ*. 644, 1391-1398. DOI: 10.1016/j.scitotenv.2018.06.324.

Ccanccapa, A., Masiá,, A., Navarro-Ortega, A., Picó, Y., Barceló, D., 2016. Pesticides in the Ebro River basin: Occurrence and risk assessment. *Environ. Pollut*. 211, 414-424, DOI: 10.1016/j.envpol.2015.12.059.

Clasen, B., Loro, V. L., Murussi, C. R., Tiecher, T. L., Moraes, B., Zanella, R., 2018. Bioaccumulation and oxidative stress caused by pesticides in Cyprinus carpio reared in a rice-fish system. *Sci. Total Environ*. 626, 737-743. DOI: 10.1016/j.scitotenv.2018.01.154.

Dimou, A. D., Sakkas, V. A., Albanis, T., A., 2004. Trifluralin photolysis in natural waters and under the presence of isolated organic matter and nitrate ions: kinetics and photoproduct analysis, *J. Photochem. Photobiol. A-Chem.* 163, 473-480. DOI: 10.1016/j.jphotochem.2004.02.001.

Dong, B., Hu, J., 2016. Photodegradation of the novel fungicide fluopyram in aqueous solution: kinetics, transformation products, and toxicity evolvement. *Environ Sci Pollut Res* 23, 19096-19106. DOI: 10.1007/s11356-016-7073-7.

551 Ecological Structure Activity Relationships (ECOSAR) Class Program - U.S. Environmental
552 Protection Agency (EPA). https://www.epa.gov/tsca-screening-tools/ecological-structure-activity-
553 relationships-ecosar-predictive-model. Last access: July 2019.
554
555 Erickson, P. R., Grandbois, M., Arnold, W. A., McNeill, K., 2012. Photochemical Formation of
556 Brominated Dioxins and Other Products of Concern from Hydroxylated Polybrominated Diphenyl
557 Ethers (OHPBDEs). *Environ. Sci. Technol*. 46, 8174−8180. DOI: 10.1021/es3016183.
558
559 Eyheraguibel, B., ter Halle, A., Richard, C., 2009. Photodegradation of Bentazon, Clopyralid, and
560 Triclopyr on Model Leaves: Importance of a Systematic Evaluation of Pesticide Photostability on
561 Crops. *J. Agric. Food Chem*. 57, 1960-1966. DOI: 10.1021/jf803282f.
562
563 Fenner, K., Canonica, S., Wackett, L. P., Elsner, M., 2013. Evaluating Pesticide Degradation in the
564 Environment: Blind Spots and Emerging Opportunities. *Science* 341, 752. DOI:
565 10.1126/science.1236281.
566
567 Galbavy, E. S., Ram, K., Anastasio, C., 2010. 2-Nitrobenzaldehyde as a chemical actinometer for
568 solution and ice photochemistry. *J. Photochem. Photobiol. A-Chem.* 209, 186-192. DOI:
569 10.1016/j.jphotochem.2009.11.013.
570
571 Guelfi, D. R. V., Brillas, E., Gozzi, F., Machulek, A., de Oliveira, S. C., Sirés, I., 2019. Influence of
572 electrolysis conditions on the treatment of herbicide bentazon using artificial UVA radiation and
573 sunlight. Identification of oxidation products. *J. Environ. Manage.* 231, 213-221. DOI:
574 10.1016/j.jenvman.2018.10.029.
575

576 Isidori, M., Parrella, A., Pistillo, P., Temussi, F., 2009. Effects of ranitidine and its photoderivatives
577 in the aquatic environment. *Environ. Int.* 35, 821-825. DOI: 10.1016/j.envint.2008.12.002.
578
579 Kanawi, E., Van Scoy, A. R., Budd, R., Tjeerdema, R. S., 2016. Environmental fate and
580 ecotoxicology of propanil: a review. *Toxicol. Environ. Chem.* 98, 689-704. DOI:
581 10.1080/02772248.2015.1133816.
582
583 Katagi., T. 2013. Aerobic microbial transformation of pesticides in surface water. *J. Pestic. Sci.* 38,
584 10–26. DOI: 10.1584/jpestics.D12-053.
585
586 Katagi, T., 2018. Direct photolysis mechanism of pesticides in water. *J Pestic Sci*. 43, 57-72. DOI:
587 10.1584/jpestics.D17-081.
588
589 Köck-Schulmeyer, M., Postigo, C., Farré, M., Barceló, D., López de Alda, M., 2019. Medium to
590 highly polar pesticides in seawater: Analysis and fate in coastal areas of Catalonia (NE Spain).
591 *Chemosphere* 215, 515-523. DOI: 10.1016/j.chemosphere.2018.10.049.
592
593 Konstantinou, I. K., Zarkadis, A. K., Albanis, T. A., 2001. Photodegradation of Selected Herbicides
594 in Various Natural Waters and Soils under Environmental Conditions. *J. Environ. Qual*. 30, 121-
595 130. DOI: 10.2134/jeq2001.301121x.
596
597 Lammoglia, S. K., Brun, F., Quemar, T., Moeys, J., Barriuso, E., Gabrielle, B., Mamy, L., 2018.
598 Modelling pesticides leaching in cropping systems: Effect of uncertainties in climate, agricultural
599 practices, soil and pesticide properties. *Environ. Modell. Softw.* 109, 342-352. DOI:
600 10.1016/j.envsoft.2018.08.007.
601

602 Leresche, F., von Gunten, U., Canonica, S., 2016. Probing the Photosensitizing and Inhibitory
603 Effects of Dissolved Organic Matter by Using N,N-dimethyl-4-cyanoaniline (DMABN). *Environ.*
604 *Sci. Technol*. 50, 10997-11007. DOI: 10.1021/acs.est.6b02868.
605
606 Liu, B., McConnell, L. L., Torrents, A., 2001. Hydrolysis of chlorpyrifos in natural waters of the
607 Chesapeake Bay. *Chemosphere* 44, 1315-1323. DOI: 10.1016/S0045-6535(00)00506-3.
608
609 Luo, Y., Guo, W., Ngo, H. H., Nghiem, L. D., Hai, F. I., Zhang, J., Liang, S., Wang, X. C., 2014. A
610 review on the occurrence of micropollutants in the aquatic environment and their fate and removal
611 during wastewater treatment. *Sci. Total Environ*. 473–474, 619-641. DOI:
612 10.1016/j.scitotenv.2013.12.065.
613
614 Lupi, L., Bedmar, F., Puricelli, M., Marino, D., Aparicio, V. C., Wunderlin, D., Miglioranza, K. S.
615 B., 2019. Glyphosate runoff and its occurrence in rainwater and subsurface soil in the nearby area
616 of agricultural fields in Argentina. *Chemosphere* 225, 906-914. DOI:
617 10.1016/j.chemosphere.2019.03.090.
618
619 Malouki, M. A., Zertal, A., Lavédrine, B., Sehili, T., Boule, P., 2004. Phototransformation of 3,5-
620 dihalogeno-4-hydroxybenzonitriles (ioxynil and chloroxynil) in aqueous solution. *J. Photochem.*
621 *Photobiol. A-Chem.* 168, 15-22. DOI: 10.1016/j.jphotochem.2004.05.007.
622
623 Marchisio, A., Minella, M., Maurino, V., Minero, C., Vione, D., 2015. Photogeneration of reactive
624 transient species upon irradiation of natural water samples: Formation quantum yields in different
625 spectral intervals, and implications for the photochemistry of surface waters. *Water Res.* 73, 145-
626 156. DOI: 10.1016/j.watres.2015.01.016.
627

628 Masiá, A., Campo, J., Navarro-Ortega, A., Barceló, D., Picó, Y., 2015. Pesticide monitoring in the
629 basin of Llobregat River (Catalonia, Spain) and comparison with historical data. *Sci. Total Environ*.
630 503–504, 58-68. DOI: 10.1016/j.scitotenv.2014.06.095.
631
632 Mayo-Bean, K., Moran, K., Meylan, B., Ranslow, P., 2012. Methodology Document for the
633 ECOlogical Structure-Activity Relationship Model (ECOSAR) Class Program. US-EPA,
634 Washington DC, 46 pp.
635
636 Mayo-Bean, K., Moran-Bruce, K., Meylan, W., Ranslow, P., Lock, M., Nabholz, J. V., Runnen, J.
637 V., Cassidy, L. M., Tunkel, J., 2017a. Methodology Document for the ECOlogical Structure-
638 Activity Relationship Model (ECOSAR) Class Program. US-EPA, Washington DC, 40 pp.
639
640 Mayo-Bean, K., Moran-Bruce, K., Nabholz, J. V., Meylan, W. M., Howard, P. H., Cassidy, L.,
641 2017b. Operation Manual for the ECOlogical Structure-Activity Relationship Model (ECOSAR)
642 Class Program. US-EPA, Washington DC, 37 pp.
643
644 McNeill, K., Canonica, S., 2016. Triplet state dissolved organic matter in aquatic photochemistry:
645 reaction mechanisms, substrate scope, and photophysical properties. *Environ. Sci.-Process Impacts*
646 18, 1381-1399. DOI: 10.1039/C6EM00408C.
647
648 Metcalfe, C. D., Helm, P., Paterson, G., Kaltenecker, G., Murray, C., Nowierski, M., Sultana, T.,
649 2019. Pesticides related to land use in watersheds of the Great Lakes basin,
650 *Sci. Total Environ.* 648, 681-692. DOI: 10.1016/j.scitotenv.2018.08.169.
651

652 Milan, M., Vidotto, F., Piano, S., Negre, M., Ferrero, A., 2012. Dissipation of Propanil and 3,4
653 Dichloroaniline in Three Different Rice Management Systems. *J. Environ. Qual.* 41, 1487-1496.
654 DOI: 10.2134/jeq2012.0175.
655
656 Milan, M., Ferrero, A., Fogliatto, S., Piano, S., Vidotto, F., 2015. Leaching of S-metolachlor,
657 terbuthylazine, desethyl-terbuthylazine, mesotrione, flufenacet, isoxaflutole, and diketonitrile in
658 field lysimeters as affected by the time elapsed between spraying and first leaching event. *J.*
659 *Environ. Sci. Heal. B* 50, 851-861, DOI: 10.1080/03601234.2015.1062650.
660
661 Mir, N. A., Haque, M. M., Khan, A., Muneer, M., Vijayalakshmi, S., 2014. Photocatalytic
662 degradation of herbicide Bentazone in aqueous suspension of TiO_2: mineralization, identification of
663 intermediates and reaction pathways. *Environ. Technol.* 35, 407-415. DOI:
664 10.1080/09593330.2013.829872.
665
666 Nilles, G. P., Zabik, M. J., 1975. Photochemistry of bioactive compounds. Multiphase
667 photodegradation and mass spectral analysis of basagran. *J. Agric. Food Chem*. 23, 410-415. DOI:
668 10.1021/jf60199a068.
669
670 O'Neil, M.J., 2013. The Merck Index - An Encyclopedia of Chemicals, Drugs, and Biologicals.
671 Cambridge, UK: Royal Society of Chemistry, p. 185.
672
673 Palma, P., Matos, C., Alvarenga, P., Köck-Schulmeyer, M., Simões, I., Barceló, D., López de Alda,
674 M. J., 2018. Ecological and ecotoxicological responses in the assessment of the ecological status of
675 freshwater systems: A case-study of the temporary stream Brejo of Cagarrão (South of Portugal).
676 *Sci. Total Environ*. 634, 394-406. DOI: 10.1016/j.scitotenv.2018.03.281.
677

678 Papadakis, E. N., Tsaboula, A., Vryzas, Z., Kotopoulou, A., Kintzikoglou, K., Papadopoulou-
679 Mourkidou, E., 2018. Pesticides in the rivers and streams of two river basins in northern Greece,
680 *Sci. Total Environ*. 624, 732-743, DOI: 10.1016/j.scitotenv.2017.12.074.
681
682 Passananti, M., Lavorgna, M., Iesce, M. R., DellaGreca, M., Brigante, M., Criscuolo, E., Cermola,
683 F., Isidori, M., 2015. Photochemical fate and eco-genotoxicity assessment of the drug etodolac. *Sci.*
684 *Total Environ*. 518-519, 258-265, DOI: 10.1016/j.scitotenv.2015.03.009.
685
686 Peschka, M., Petrovic, M., Knepper, T. P., Barceló, D., 2007. Determination of two
687 phototransformation products of bentazone using quadrupole time-of-flight mass spectrometry.
688 *Anal. Bioanal. Chem.* 388, 1227–1234. DOI 10.1007/s00216-007-1349-1.
689
690 Ramesh, A., Balasubramanian, M., 1999. Kinetics and Hydrolysis of Fenamiphos, Fipronil, and
691 Trifluralin in Aqueous Buffer Solutions. *J. Agric. Food Chem*. 47, 3367-3371. DOI:
692 10.1021/jf980885m.
693
694 Remucal, C. K., 2014. The role of indirect photochemical degradation in the environmental fate of
695 pesticides: a review. *Environ. Sci.-Process Impacts*16, 628-653. DOI: 10.1039/C3EM00549F.
696
697 Riise, G., Lundekvam, H., Wu, Q., Haugen, L. E., Mulder, J., 2004. Loss of Pesticides from
698 Agricultural Fields in SE Norway – Runoff Through Surface and Drainage Water. *Environ.*
699 *Geochem. Health.* 26, 269-276. DOI: 10.1023/B:EGAH.0000039590.84335.d6.
700
701 Roehrs, R., Roehrs, M., Machado, S. L., Zanella, R., 2012. Biodegradation of Herbicide Propanil
702 and Its Subproduct 3,4-Dichloroaniline in Water. *Clean-Soil Air Water* 40, 958-964. DOI:
703 10.1002/clen.201100693.

Rose, K. C., Williamson, C. E., Saros, J. E., Sommaruga, R., Fischerd, J., M., 2009. Differences in UV transparency and thermal structure between alpine and subalpine lakes: implications for organisms. *Photochem. Photobiol. Sci.* 8, 1244-1256. DOI: 10.1039/B905616E.

Silva, E., Daam, M. A., Cerejeira, M. J., 2015. Aquatic risk assessment of priority and other river basin specific pesticides in surface waters of Mediterranean river basins. *Chemosphere*, 135, 394-402. DOI: 10.1016/j.chemosphere.2015.05.013.

Song, S., Zhang, C., Chen, Z., Wei, J., Tan, H., Li, X., 2019. Hydrolysis and photolysis of bentazone in aqueous abiotic solutions and identification of its degradation products using quadrupole time-of-flight mass spectrometry. *Environ. Sci. Pollut. Res.* 26, 10127-10135. DOI: 10.1007/s11356-019-04232-z.

Tebes-Stevens, C., Patel, J. M., Jones, W. J., Weber, E. J., 2017. Prediction of Hydrolysis Products of Organic Chemicals under Environmental pH Conditions. *Environ. Sci. Technol*. 51, 5008-5016. DOI: 10.1021/acs.est.6b05412.

Vione, D., Minella, M., Maurino, V., Minero, C., 2014. Indirect photochemistry in sunlit surface waters: Photoinduced production of reactive transient species. *Chem. Eur. J*. 20, 10590–10606. DOI: 10.1002/chem.201400413.

Vogna, D., Marotta, R., Andreozzi, R., Napolitano, A., d'Ischia, M., 2004. Kinetic and chemical assessment of the UV/H_2O_2 treatment of antiepileptic drug carbamazepine. *Chemosphere* 54, 497-505. DOI: 10.1016/S0045-6535(03)00757-4.

730 Walse, S. S., Morgan, S. L., Kong, L., Ferry, J. L., 2004. Role of Dissolved Organic Matter, Nitrate,
731 and Bicarbonate in the Photolysis of Aqueous Fipronil. *Environ. Sci. Technol*. 38, 3908-3915. DOI:
732 10.1021/es0349047.
733
734 Wenk, J., Canonica, S., 2012. Phenolic Antioxidants Inhibit the Triplet-Induced Transformation of
735 Anilines and Sulfonamide Antibiotics in Aqueous Solution. *Environ. Sci. Technol*. 46, 10, 5455-
736 5462. DOI: 10.1021/es300485u.
737
738 White, R. C., Oppliger, K. D., Johnson, J. E., 1996. The photochemistry of amides and amide
739 derivatives 3: The photolysis of methyl-2-phenoxybenzohydroxamate. *J. Photochem. Photobiol. A-*
740 *Chem.*, 101, 197-200. DOI: 10.1016/S1010-6030(96)04416-4.
741
742 Willett, K. L., Hites, R. A., 2000. Chemical Actinometry: Using o-Nitrobenzaldehyde to Measure
743 Lamp Intensity in Photochemical Experiments. *J. Chem. Educ*. 77, 900-902. DOI:
744 10.1021/ed077p900.
745
746 Williams, K. L., Tjeerdema, R. S., 2016. Hydrolytic Activation Kinetics of the Herbicide
747 Benzobicyclon in Simulated Aquatic Systems. *J. Agric. Food Chem*. 64, 4838-4844. DOI:
748 10.1021/acs.jafc.6b00603.
749
750 Zeng, T., Arnold, W. A., 2013. Pesticide Photolysis in Prairie Potholes: Probing Photosensitized
751 Processes. *Environ. Sci. Technol*. 47, 6735-6745. DOI: 10.1021/es3030808.